International Journal of Chemistry Research
Vol 1, Issue 1, 2010

Research Article

SPECTROSCOPIC AND STATISTICAL ANALYSIS ON CANCEROUS HUMAN BREAST TISSUES

G.DEVI[1], T. S. RENUGA DEVI[2] AND S.GUNASEKARAN[3]

[1]Department of Physics, R.M.K. College of Engineering and Technology, Puduvoyal, [2]PG Department of Physics, Women's Christian College, Chennai, [3]Registrar, Periyar University, Salem. Email: devi_renuga@yahoo.com, devinivash@gmail.com

Received: 24 April 2010, Revised and Accepted: 12 May 2010

ABSTRACT

The sensitivity of FTIR spectroscopy for biomolecular changes is used to classify benign and malignant breast tissues. The analysis is carried out for a collection of 43 samples which were histopathologically identified as normal, hyperplasia, fibro adenoma, ductal carcinoma and invasive ductal carcinoma tissues. In the present chapter the infrared spectra of human breast tissues were analyzed in the frequency range between 1100 cm^{-1} and 2100 cm^{-1}.The selected areas indicate the amide I and amide III bands corresponding to vibrational modes of the peptide bonds of the secondary structure of proteins. Some remarkable spectral differences were observed among normal, hyperplasia, fibro adenoma, ductal carcinoma and invasive ductal carcinoma tissues. The significant absorption bands which differentiate the different cancer grades were found to be at 1260 cm^{-1}, 1304 cm^{-1},1446 cm^{-1} ,1657 cm^{-1}, 1746 cm^{-1} 2028 cm^{-1} ,2062 cm^{-1} ,2084 cm^{-1}. The difference in the absorbance values or the various cancer grades is compared using the Trend analysis. Thus it implies that FTIR spectroscopy is useful for the diagnosis of cancerous breast tissues.

Keywords: FTIR spectroscopy, breast tissues, ductal carcinoma, amide I and amide III bands, Trend analysis

INTRODUCTION

The breast cancer is the most common malignant tumor found in women in the Western world.Usually, the breast cancer screening involves two steps. The first one is the search for palpable lesions in the annual clinical breast examination. The second one is the X- ray mammography, in which suspicious local density changes could be detected. Whenever the tissue is particularly dense throughout, ultrasound may also be used to locate suspicious regions. If a lesion is found during examination the tissue is submitted to biopsy that could ranges from the needle aspiration of single cells to the surgical removal of the entire suspicious mass by exsisional biopsy.[1-4] The breast is a large secretory gland composed of 15 to 25 autonomous and empty lobes connected to the nipple. The lobes themselves are divided into smaller units, called lobules, which are connected by ducts. Lobular and duct elements consists of single layers of epithelial and myothelial cells The breast undergoes many changes throughout a women's life, both progressive due to puberty, pregnancy and menopause and cyclical due to menstruation. Hormones regulate these changes.[5,6] This dynamical activity could induce a lot of opportunities for disease. Usually, breast pathology is extremely diverse, but it could be divided inti two main categories: benign and malignant pathologies. Most benign lesions are part of a spectrum of fibrocystic changes, where as 70% of malignant lesions are invasive duct carcinomas.[7,8]

This chapter focuses on the FTIR spectra covering the region between 1100 cm-1 and 2100 cm-1.The study of the spectra enables to identify the spectroscopic differentiation among the various breast carcinoma types namely hyperplasia, fibro adenoma, ductal carcinoma and invasive ductal carcinoma. The analysis is done using the statistical methods TREND ANALYSIS method.

MATERIALS AND METHODS

Human breast tissues were obtained from pathology department at Government General Hospital, Madras Medical College, and Chennai. Each sample was cut into two pieces. The first one was sent to the pathologists for evaluation using their histopathological techniques. The second was frozen in saline water immediately after collecting it and used for IR spectroscopic recording within few hours. For FTIR spectroscopic recording the frozen tissues was taken as thin layer and dried then placed on the BaF_2 window in the spectrophotometer. Totally about 43 samples were collected. Among those 43 samples 10 were diagnosed as infiltrating ductal carcinoma, 10 as ductal carcinoma, 9 as fibro adenoma, 9 as hyperplasia and 5 as normal breast tissues.

RESULTS AND DISCUSSION

The representative graph of the FTIR spectra of the normal, hyperplasia, fibroadenoma, ductal carcinoma and invasive ductal carcinoma is shown in the figure 1. The absorption band at 1446 cm-1corresponds tro the C-H deformation mode of methylene group.. The area between 1200 cm-1 and 1800 cm-1 indicate the amide I and amide –II bands corresponding to vibrational modes of the peptide bonds of the secondary structure of proteins. The amide –I band corresponds to vibration of C, O and H atoms in the –CONH – group. The amide –III band involves the motion of C- radical, C-N and N-H groups. [9, 10, 11]

The spectral differences show the measurable gifferences in the secondary structure of proteins of breast tissues that could differentiate subtypes of malignant lesions, as ductal carcinoma –in-situ and invasive ductal carcinoma. Thus the spectral difference is used to quantify the degree of pathogenicity of breast cancer.

The peaks in the region of 1304 cm-1 - 1310 cm-1, 1446 cm-1 and 1657 cm-1 - 1660 cm-1 are vibrational modes of adenine, cystosine, collgen, lipids, carbohydrates, proteins and pentoses respectively. The absorbance difference could be related to the presence of necrosis and lymphocytes in the tissue with necrosis. The lymphocytes appear due to the inflammatory process in this tissue sample. Thus, this spectral region could be useful to diagnose the presence of necrosis in breast cancer tissues. [12, 13]

The peak at 2048 and the peak at 2084 cm-1 are related to the C ≡ C bonds that could be present in unsaturated fatty acids, lipids and steroids.

Comparative analysis of various breast cancer grades using TREND ANALYSIS PLOT method

The statistical method used here for the variation of the absorbance values with the cancer grade is done by Trend analysis plot. Trend analysis fits a general trend model to the absorbance value. There are linear, quadratic, exponential growth or decay and s- curve models. In this method there are three accuracy measures named MAPE, MAD, and MSD. Mean Accurate Percentage Error (MAPE) measures the accuracy of fitted line series values. It measures accuracy as a percentage. Mean Absolute Deviation (MAD) measures the accuracy of fitted line series values. It expresses the accuracy in the same units as the data which helps conceptualize the amount of error. Mean Squared Deviation (MSD) is a more sensitive measure of an unusually large forecast error than MAD. The Trend analysis draws a graph containing the observations, predicted values (the

fitted trend equation) and forecast. The predicted value for a cancer grade is obtained by simple calculations using the fitted equation.

- Black symbols – observed (actual) values, Red symbols – fitted values, Green symbols – forecasts.

The trend analysis procedure also displays along with the graph, three measures to determine the accuracy of the fitted values: MAPE, MAD and MSD. These three measures are used to compare the fits obtained by using different trend models. For all three measures, smaller values generally indicate a better fitting model.

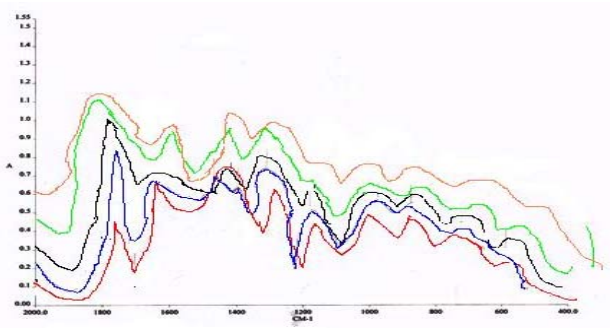

Fig. 1: Representative graph of the FTIR spectra of the normal, hyperplasia, fibro adenoma, ductal carcinoma and invasive ductal carcinoma (top to bottom)

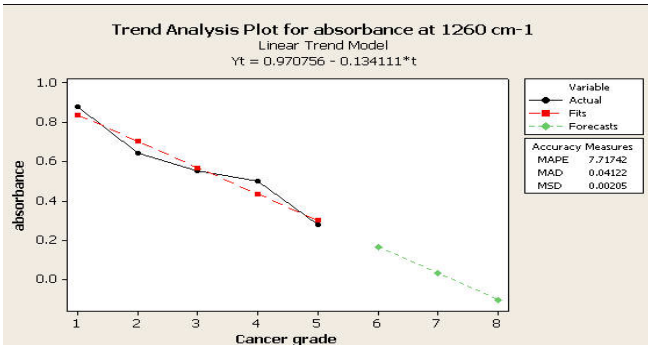

Fig 2: Trend analysis for absorbance at 1260 cm^{-1}

Trend analysis for absorbance

Fitted trend equation: Yt = 0.970756 - 0.134111*t

Accuracy measures

MAPE	7.71742
MAD	0.04122
MSD	0.00205

Forecasts

Period	**Forecast**
6	0.166089
7	0.031978
8	-0.102133

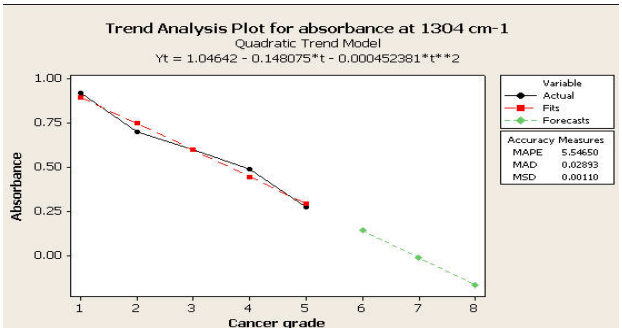

Fig. 3: Trend analysis for absorbance at 1304 cm^{-1}

Trend analysis for absorbance

Fitted trend equation: Yt = 1.04642 - 0.148075*t - 0.000452381*t**2

Accuracy measures

MAPE	5.54650
MAD	0.02893
MSD	0.00110

Forecasts

Period	**Forecast**
6	0.141689
7	-0.012267
8	-0.167127

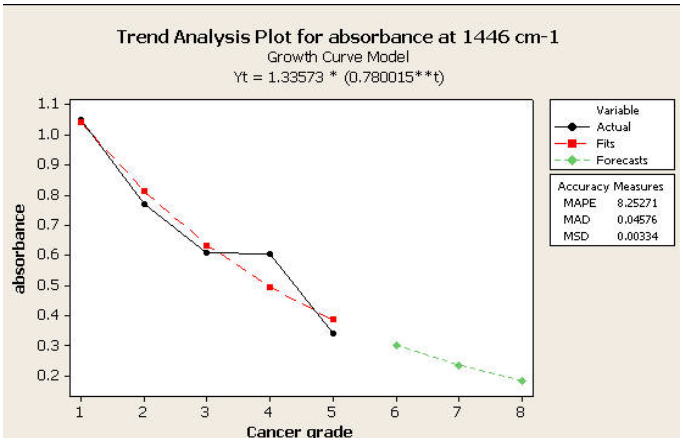

Fig. 4: Trend analysis for absorbance at 1446 cm^{-1}

Trend analysis for absorbance

Fitted trend equation: Yt = 1.33573 * (0.780015**t)

Accuracy measures

MAPE	8.25271
MAD	0.04576
MSD	0.00334

Forecasts

Period	**Forecast**
6	0.300840
7	0.234660
8	0.183038

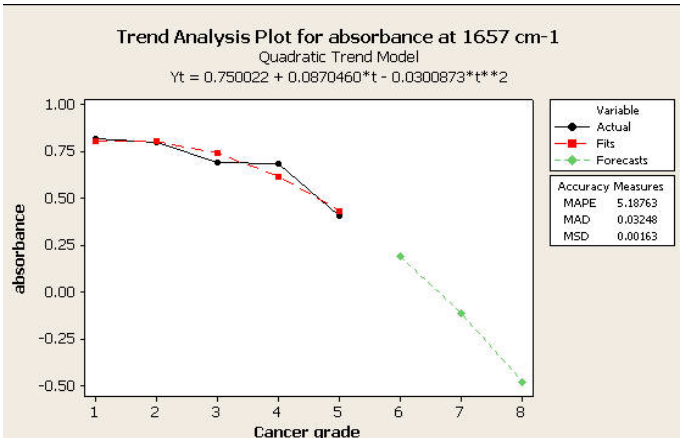

Fig. 5: Trend analysis for absorbance at 1657 cm^{-1}

Trend analysis Plot for absorbance

Fitted trend equation: Yt = 0.750022 + 0.0870460*t - 0.0300873*t**2

Accuracy measures

MAPE	5.18763
MAD	0.03248
MSD	0.00163

Forecasts

Period	**Forecast**
6	0.189156
7	-0.114933
8	-0.479197

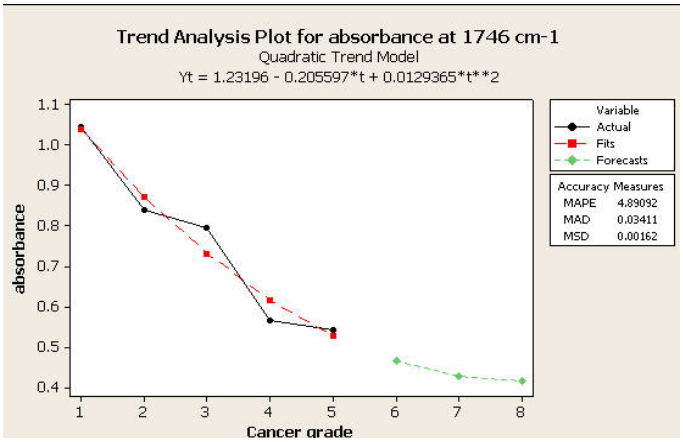

Fig. 6: Trend analysis for absorbance at 1746 cm^{-1}

Trend analysis plot for absorbance

Fitted trend equation: Yt = 1.23196 - 0.205597*t + 0.0129365*t**2

Accuracy measures

MAPE	4.89092
MAD	0.03411
MSD	0.00162

Forecasts

Period	**Forecast**
6	0.464089
7	0.426667
8	0.415117

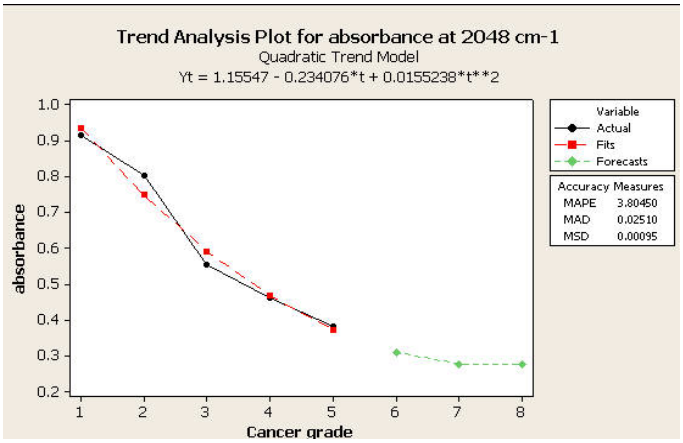

Fig. 7: Trend analysis for absorbance at 2048 cm^{-1}

Trend analysis plot for absorbance

Fitted trend equation: Yt = 1.15547 - 0.234076*t + 0.0155238*t**2

Accuracy measures

MAPE	3.80450
MAD	0.02510
MSD	0.00095

Forecasts

Period	**Forecast**
6	0.309867
7	0.277600
8	0.276381

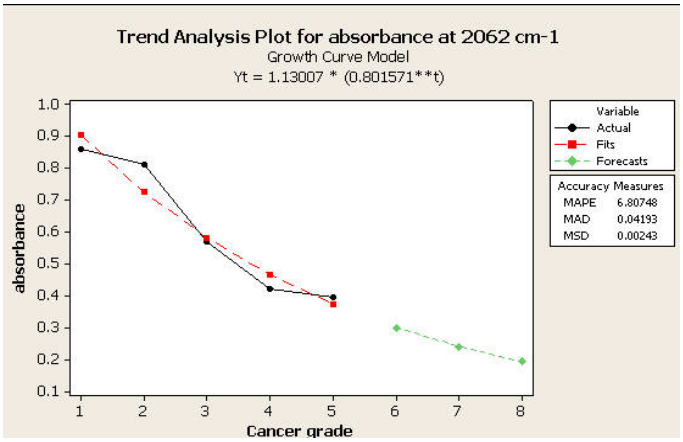

Fig. 8: Trend analysis for absorbance at 2062 cm^{-1}

Trend analysis Plot for absorbance

Fitted trend equation: Yt = 1.13007 * (0.801571**t)

Accuracy measures

MAPE	6.80748
MAD	0.04193
MSD	0.00243

Forecasts

Period	**Forecast**
6	0.299749
7	0.240270
8	0.192593

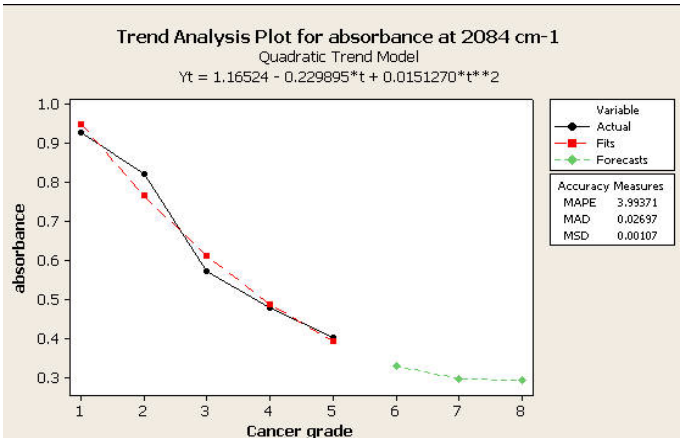

Fig. 9: Trend analysis for absorbance at 2062 cm^{-1}

Trend analysis Plot for absorbance

Fitted trend equation: Yt = 1.16524 - 0.229895*t + 0.0151270*t**2

Accuracy measures

MAPE	3.99371
MAD	0.02697
MSD	0.00107

Forecasts

Period	**Forecast**
6	0.330444
7	0.297200
8	0.294210

An individual plot illustrates both a measure of central tendency and variability of the absorbance among individual samples for each cancer grade. The individual plot of normal tissues, hyperplasia, fibro adenoma, ductal carcinoma and invasive ductal carcinoma breast tissues at 1260 cm^{-1}, 1304 cm^{-1},1446 cm^{-1}, 1657 cm^{-1} ,1746 cm^{-1} ,2048 cm^{-1}, 2062cm^{-1} and 2084 cm^{-1} are shown in fig-(2-6) respectively. The interval plot for the regions between 1260 cm^{-1} and 2084 cm^{-1} clearly shows that the absorbance values for the benign breast tissues have a higher value compared to the malignant breast tissues.

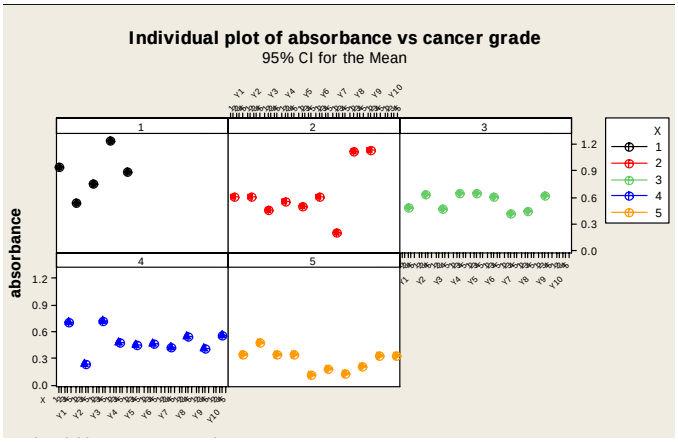

Fig. 10: Individual plot of absorbance vs. cancer grades for the region 1260 cm^{-1}(1-normal, 2- hyperplasia, 3- fibroadenoma, 4- ductal)carcinoma 5- invasive ductal carcinoma)

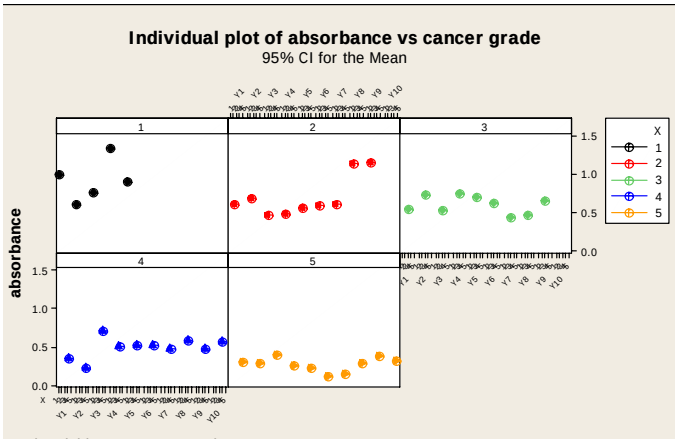

Fig. 11: Individual plot of absorbance vs. cancer grades for the region 1304 cm^{-1}(1-normal, 2- hyperplasia, 3- fibroadenoma, 4- ductal carcinoma, 5-invasiveductalcarcinoma)

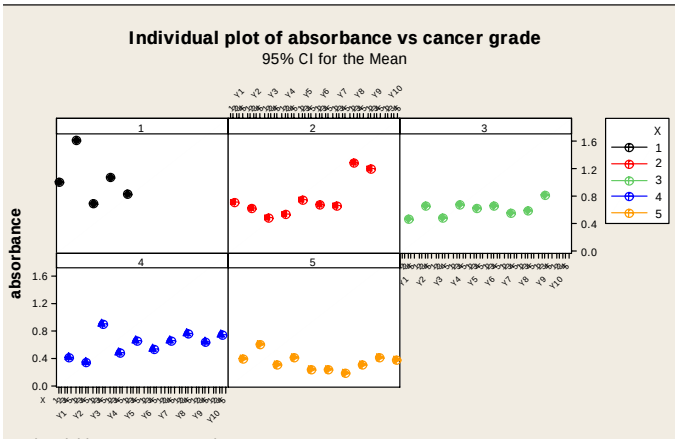

Fig. 12: Individual plot of absorbance vs. cancer grades for the region 1446 cm^{-1}(1-normal, 2- hyperplasia, 3- fibroadenoma, 4- ductal carcinoma, 5-invasiveductalcarcinoma)

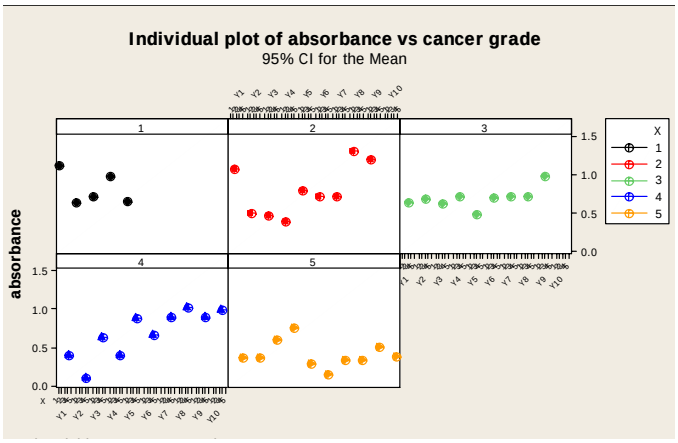

Fig. 13: Individual plot of absorbance vs. cancer grades for the region 1657cm^{-1}(1-normal, 2- hyperplasia, 3- fibroadenoma, 4- ductal carcinoma, 5-invasiveductalcarcinoma)

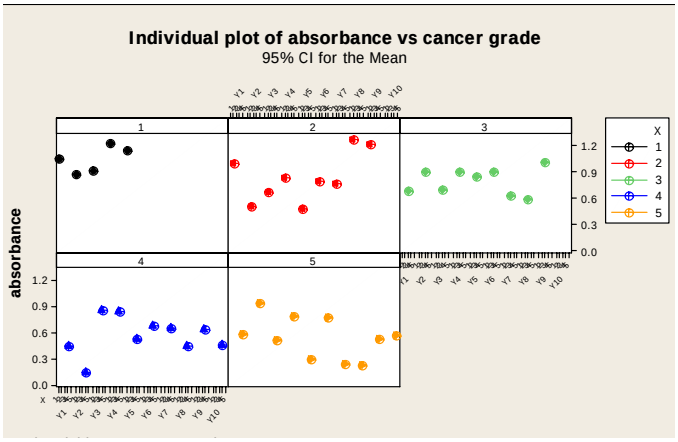

Fig. 14: Individual plot of absorbance vs. cancer grades for the region1746 cm^{-1}(1-normal, 2- hyperplasia, 3- fibroadenoma, 4- ductal carcinoma, 5-invasiveductalcarcinoma)

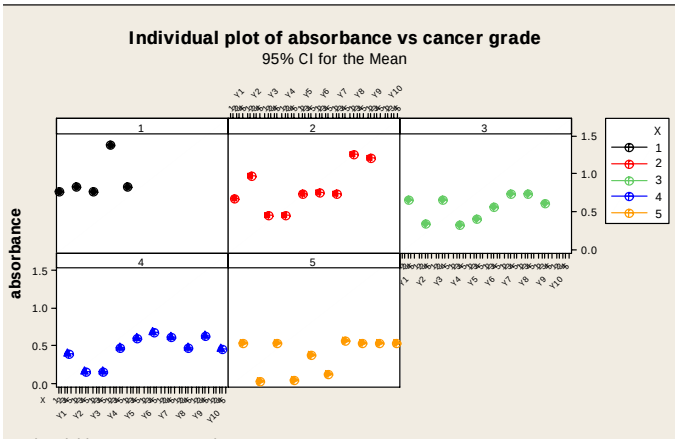

Fig. 15: Individual plot of absorbance vs. cancer grades for the region2048 cm^{-1}(1-normal, 2- hyperplasia, 3- fibroadenoma, 4- ductal carcinoma, 5-invasiveductalcarcinoma)

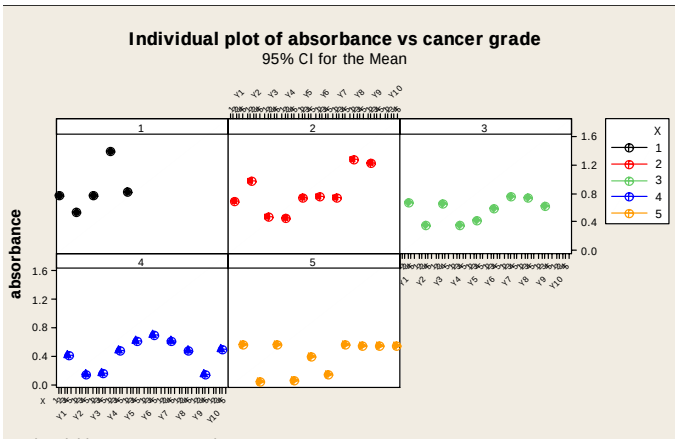

Fig. 16: Individual plot of absorbance vs. cancer grades for the region2062 cm^{-1}(1-normal,2-hyperplasia,3-fibroadenoma,4-ductalcarcinoma,5-invasiveductalcarcinoma)

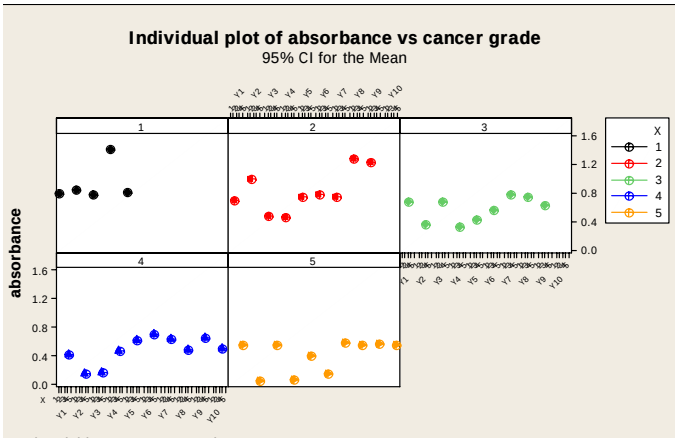

Fig. 17: Individual plot of absorbance vs. cancer grades for the region 2084cm^{-1}(1-normal, 2- hyperplasia, 3- fibroadenoma, 4- ductal carcinoma, 5-invasiveductal carcinoma)

CONCLUSION

In this study it has been analyzed that the Infra Red spectra differentiated the normal and tumoral breast tissues including hyperplasia, fibro adenoma, ductal carcinoma and invasive ductal carcinoma. The collected samples were histopathologically classified into five groups. The FTIR spectrum of all the above said categories of breast cancerous tissues shows that the specific regions at 1260

cm^{-1}, 1304 cm^{-1}, 1446 cm^{-1}, 1657 cm^{-1}, 1746 cm^{-1},2048 cm^{-1},2062 cm-1,2084 cm^{-1} there were some remarkable differences in the absorbance values. This difference is because of the changes in the proteins due to the cell proliferation in the carcinogenesis process. This difference in the absorbance values for various categories of the tissue samples was well defined by the names trend analysis plot. The plot explains the trend in the variation of the absorbance for various cancer grades. The forecasts clearly establish the carcinogenesis process when absorbance values reach an extreme smaller value. The individual plot also confirms the fact that the absorbance of normal breast tissues has a higher value compared to malignant tissues for all the above said frequency regions.The changes in the absorbance values for the different cancer grades were because of the changes in the biomolecular changes in the tissues. Thus FTIR has a great role in the qualitative analysis of cancerous breast ti**ss**ues**.**

REFERENCES

1. Noguchi M: Therapeutic relevance of breast cancer micrometastases in sentinel lymph nodes. *Br J Surg* 2002, 89:1505-1515.
2. Sitter B, Sonnewald U, Spraul M, Fjosne HE, Gribbestad IS: High-resolution magic angle spinning MRS of breast cancer tissue. *NMR Biomed* 2002, 15:327-337.
3. Specht DF: Probabilistic neural networks. *Neural Network* 1990, 3:109-118.
4. American Cancer Society: Cancer Facts and Figures 2007. American Cancer Society (2007).
5. U. S. Cancer Statistics Working Group: United states cancer statistics: 2003 incidence and mortality (preliminary data). National Vital Statistics 53(5) (2004).
6. Rosai, J.: Rosai and Ackerman's Surgical Pathology. 9th edn. Mosby (2004).
7. Suri, J.S., Rangayyan, R.M.: Recent Advances in Breast Imaging, Mammography, and Computer-Aided Diagnosis of Breast Cancer. 1st edn. SPIE (2006).
8. Hoos, A., Cordon-Cardo, C.: Tissue microarray profiling of cancer specimens and cell lines: Opportunities and limitations. Mod. Pathol. 81(10), 1331–1338 (2001).
9. Lekadir, K., Elson, D.S., Requejo-Isidro, J., Dunsby, C., McGinty, J., Galletly, N., Stamp, G., French, P.M., Yang, G.Z.: Tissue characterization using dimensionality reduction and fluorescence imaging. In: Larsen, R., Nielsen, M., Sporring, J. (eds.) MICCAI 2006. LNCS, vol. 4191, pp. 586–593. Springer, Heidelberg (2006).
10. Oliver, A., Freixenet, J., Marti, R., Zwiggelaar, R.: A comparison of breast tissue classification techniques. In: Larsen, R., Nielsen, M., Sporring, J. (eds.) MICCAI 2006. LNCS, vol. 4191, pp. 872–879. Springer, Heidelberg (2006).
11. Rodan SB, Rodan GA: Integrin function in osteoclasts. *Endocrinol* 1997,4**(**Suppl)**:**S47-56.
12. Hill PA, Docherty AJP, Bottomley KMK, O'Connell JP, Morphy JR, Reynolds JJ, Meikle MC: Inhibition of Bone Resorption In Vitro by Selective Inhibitors of Gelatinase and Collagenase**.** *Biochem J* 1995, 308:167-175.
13. Pei D, Weiss SJ: Transmembrane deletion mutants of the membrane-type matrix metalloproteinase-1 activate progelatinase A and express intrinsic matrix-degrading activity. *J Biol Chem* 1996, 271**:**9135-9140.